Collective charge-density excitations in two-component one-dimensional quantum plasmas: Phase-fluctuation-mode dispersion and spectral weight in semiconductor quantum-wire nanostructures

S. Das Sarma and E. H. Hwang

Department of Physics, University of Maryland, College Park, Maryland 20742-4111

Collective charge-density excitation spectra of both a spatially separated two-component quasi-one-dimensional (1D) quantum plasma, as existing in a semiconductor double quantum-wire structure, and a 1D homogeneous electron-hole plasma, as appropriate for a photoexcited semiconductor quantum-wire system, are calculated within the two-component random-phase approximation. We find two phase-fluctuation collective modes, one (optical plasmon, OP) with energy proportional to $q|\ln(qa)|^{1/2}$ is the *total* in-phase (out-of-phase) charge-density oscillation of the system and the other (acoustic plasmon, AP) with a linear energy dispersion as $q \to 0$ is the *neutral* out-of-phase (in-phase) charge-density oscillation of the system for the situation where the two components have the same (opposite) charges, where q is the 1D wave vector and a is a characteristic 1D confinement size. In contrast to higher dimensional systems we find the neutral long wavelength AP mode to be generically undamped by Landau damping effects due to the severe suppression of single-particle excitations in 1D systems. We also investigate the effect of impurity scattering on the collective-mode dispersion and damping, and calculate the collective-mode spectral weight by obtaining the dynamical structure factor. We find that both OP and AP modes are overdamped by impurity scattering below some critical wave vector. We find that in the long wavelength limit the spectral weight is carried mostly by the OP, but the spectral weight of the undamped AP mode at finite (but not too large) wave vectors is comparable with that of the OP mode, making it viable to observe the AP mode in semiconductor quantum-wire systems. The effect of the interwire electron tunneling in a biwire system on the collective charge density excitation spectra is also studied. We discuss the mode dispersion and damping from an effective Luttinger liquid perspective as well and in some cases include local-field corrections in our calculations. [S0163-1829(99)09115-8]

I. INTRODUCTION

Recent advances in fabrication techniques involving molecular-beam epitaxy and lithography have now made it possible to make narrow GaAs-based quasi-one-dimensional (1D) electronic systems with lateral dimensions of the order of the Bohr radius.[1] In these so-called quantum-wire structures, the motion of charge carriers is confined in two transverse directions but is essentially free (in the effective-mass sense) in the longitudinal direction. Study of collective modes in reduced dimensional electron systems in semiconductor nanostructures is a subject of growing experimental and theoretical interest. Experimentally, far-infrared optical spectroscopy[2,3] and resonant inelastic light-scattering spectroscopy[4–6] have been used to study quasi-1D elementary electronic excitations. Several theoretical studies, mostly based on the random-phase approximation (RPA), have been reported on the energy dispersion of elementary excitations in semiconductor quantum wires. The measured 1D intrasubband plasmon dispersion agrees remarkably well with the RPA predictions.[7] The quantitative agreement between RPA predictions and the experimental results[6] was later explained by the fact[8] that the calculated RPA plasmon dispersion and the Tomonaga-Lutinger theory for the collective charge-density excitations of the 1D electron system are equivalent at long wavelengths by virtue of the vanishing of vertex corrections[9] in the irreducible polarizability of the 1D electron gas.

The two-component quasi-1D systems which are composed of electrons and holes have been generated in a wide variety of semiconductor quantum wires by optical pumping. Spatially separated two-component quasi-1D systems can be produced by additional lateral confinement to produce a double quantum-wire structure in GaAs-Ga$_x$Al$_{1-x}$As double quantum well systems. The collective modes of the two-component plasma also play important roles in the many-body physics of carriers such as screening of the Coulomb interaction potential and in Coulomb drag problem. In this paper, we calculate the dispersion and the spectral weight of longitudinal collective modes (with and without spatial separation) in quasi-1D two-component plasmas as in semiconductor double quantum-wire structures or in photoexcited homogeneous 1D electron-hole plasmas (EHP). Our theory is based mostly on the two-component RPA (which should be well-valid in 1D systems); in the 1D EHP case we go beyond RPA to include local-field corrections to assess the validity of 1D RPA. The collective modes of the two-component plasma have been widely studied in higher dimension,[10–12] and recently, in quasi-1D two-component systems.[13]

It is well known that a two-component plasma has two branches of longitudinal collective excitation spectra called the optical plasmon (OP) and the acoustic plasmon (AP), where the density fluctuations in each component oscillate in phase (OP) and out of phase (AP), respectively, relative to each other, assuming the two charge components to be the

same. As expected, we find two plasma modes in the two-component 1D system; the in-phase OP with a typical 1D plasmon dispersion with the frequency proportional to $q|\ln(qa)|^{1/2}$ at long wavelengths and the out-of-phase AP with its frequency linear in q as $q \rightarrow 0$, where q is the 1D wave vector and a is a characteristic 1D confinement size (i.e., roughly the wire width). Unlike 2D and 3D systems, where the electron-hole pair continua have only an upper boundary, $qv_F + q^2/2m$, the 1D pair continuum has also a low-energy gap under the lower boundary $|qv_F - q^2/2m|$, implying no low-energy single-particle excitations (SPE) are allowed in 1D. This gap, the nonexistence of low-energy SPE in 1D Fermi systems, arises from severe phase-space restrictions (Pauli exclusion principle) imposed by 1D energy-momentum conservation, and leads to the possibility of the existence of an undamped plasmon mode in multicomponent 1D systems.[14] We find a low-energy undamped AP mode in the double quantum-wire system for arbitrary interwire separations (including the zero separation case). In general, in higher dimensions, the collective-mode spectral weight is mostly carried by the OP, which makes the experimental observation of the AP mode in higher dimensions rather difficult. In contrast, we find that in quasi-1D systems the spectral weight of the undamped AP mode is comparable to that of the OP mode and the spectral weight of the AP mode increases as the spatial separation increases, which is similar to the corresponding 2D situation. The greater relative spectral weight of the AP mode in 1D is directly related to the nonexistence of low-energy 1D SPE.

The plasma modes in 1D systems have vanishing frequencies at long wavelengths, and in general their energies at experimentally accessible wave vectors are small (≈ 1 meV). Their observability therefore depends rather crucially on the absence of appreciable damping or broadening in the system. While the absence of long wavelength Landau damping (to SPE) makes it feasible to discuss the observability of the AP mode, one must also have very small impurity broadening in order for the plasmon modes to be observable. Impurity scattering causes the carrier motion to be diffusive assuming the scattering to be weak. In principle, any impurity disorder, no matter how weak, localizes all single electron 1D states; for weak disorder, however, the localization length is larger than the system size and electron dynamics could be considered to be diffusive. The diffusive nature of the electronic dynamics strongly affects the plasmon dispersion in the long wavelength limit because the plasma frequency is vanishingly small at long wavelengths.[15–17] The 1D plasmons therefore become over-damped due to impurity scattering induced level broadening at sufficiently long wavelengths. This plasmon level broadening may actually play a significant role in determining the physical characteristics in quantum wires. The collisional damping of the plasmon modes due to impurity scattering occurs in addition to the Landau damping which arises from the decay of the plasmon to SPE electron-hole pair excitations. (As emphasized above, while Landau damping is suppressed in 1D, impurity broadening is always present unless the system is perfectly pure.) In the single-component plasma, it is known that, as the impurity scattering increases, the collisional damping becomes strong and the plasmon mode becomes overdamped and disappears at small q in 1D

and 2D systems (by contrast, this is a small effect in 3D since the plasmon energy is finite at zero wave vector).[15] Inclusion of impurity scattering in 1D and 2D overdamps the plasmon below a critical wave vector.[15–17] This disappearance of the plasmon spectral weight at small q has important consequences for the existence and characteristics of the Fermi surface in a one-dimensional electron gas.[16] In this paper we investigate the plasmon damping of the two-component 1D plasma in the presence of impurity scattering. (As noted above, any finite impurity disorder leads to Anderson localization of 1D one-electron states, and therefore the 1D electron dynamics in the presence of impurity disorder is exponentially localized, *not* diffusive—this is, however, a purely academic point of little relevance to high quality GaAs quantum-wire systems with low disorder, where the localization lengths are many microns long and are in fact longer than the 1D sample lengths;[18] we are therefore justified in treating the effective electron dynamics as being diffusive, neglecting the Anderson localization effects in high quality quantum wires of relevance to plasmon experiments.)

We also discuss the effect of interwire electron tunneling on the biwire collective-mode spectra. The most important qualitative feature of the plasmon dispersion in the presence of interwire tunneling is that, even though the in-phase OP mode ω_+ depends weakly on the tunneling, the out-of-phase AP mode ω_-, which is purely acoustic in the absence of tunneling ($\omega_- \sim q$), develops a plasmon gap at $q = 0$ in the presence of nonzero tunneling; the plasmon gap in the AP depends nontrivially on the 1D electron density n, the interwire tunneling amplitude t, and the interwire distance d. Tunneling therefore effectively changes the AP ($\omega_- \sim q$) into an optical mode with a long wavelength gap.

We use the RPA for most of our calculations. As emphasized, RPA is a very good approximation for the collective-mode dispersion in 1D quantum-wire structures by virtue of the essential vanishing of all vertex corrections to the 1D polarizability function. We consider the zero-temperature case and assume that our quasi-1D system has an infinite square-well confinement with a finite width a in the y direction and a zero width in the z direction. It is easy to include a finite width in the z direction but our results do not change qualitatively. In typical quantum wires, the wire width along the growth direction (z direction) is much smaller (by an order of magnitude) than that in the lateral direction (y direction), justifying our 2D finite width model for the 1D wire. In the finite width 2D model we use a square-well confining potential with infinite barriers at $y = -a/2$ and $y = a/2$, with the electron dynamics along the x axis being free. Confinement of the electrons in the y and z directions leads to the quantization of energy levels into different 1D subbands, and we assume the 1D extreme quantum limit where only the lowest subband is occupied by carriers, and all the 1D higher subbands are neglected. We study the plasmon modes of the spatially separated two-component system by taking two identical parallel quantum wires separated by a distance d. We include results for the case $d = 0$ because it applies directly to the photoexcited 1D EHP where electrons and holes are not spatially separated. We consider two different spatial configurations for our two-component biwire structure: two 1D wires with a spatial separation d being parallel to each other aligned in the (1) x-z plane (separated

along the y axis) and (2) x-y plane (separated along the z axis). Since the difference in our calculated results between these two configurations is within 1%, we only give the results for the configuration (1).

It is well known that 1D electron systems are fundamentally different from their higher dimensional counterparts because 1D interacting electrons form a Luttinger liquid, not a Fermi liquid, and any electron-electron interaction, no matter how weak, destroys the Fermi surface, i.e., the discontinuity in the momentum distribution function, in 1D. It turns out, however, that this distinction, while being profound at a fundamental theoretical level (because it implies the nonexistence of quasiparticles in 1D systems), is rather irrelevant to the understanding of the collective-mode spectra and their experimental realization in semiconductor quantum-wire structures. As has been emphasized elsewhere, RPA gives a very good account of the collective-mode properties in 1D semiconductor quantum-wire structures, and we discuss this issue in some detail in this paper in the context of the two-component 1D plasma.

The rest of the paper is organized as follows: In Sec. II we provide the basic RPA formalism as well as the calculated analytic and numerical results for plasmon dispersion, damping, and spectral weight by obtaining the dynamical structure factor (which is a direct measure of the light-scattering intensity); in Sec. III we study the effects of the interwire electron tunneling in a biwire system on the collective charge density excitation spectra; in Sec. IV the plasmon dispersion and damping in the photoexcited 1D EHP is studied in both RPA and including local-field corrections; in Sec. V we briefly discuss the acoustic plasmon mode of the two-component 1D Luttinger liquid; we conclude in Sec. VI providing a brief summary of our results.

II. RPA THEORY AND RESULTS

In general, the density-fluctuation spectra or the plasmons or the longitudinal collective modes of a solid-state plasma are given by the poles of the density-density correlation function, or equivalently by the zeros of the dynamical dielectric function. For a multicomponent plasma the collective modes are given by the zeros of the generalized dielectric tensor ϵ. In the two-component spatially separated 1D plasma the generalized dielectric tensor with wire indices i,j ($=1,2$ indicating the two quantum wires) is given (neglecting any interwire tunneling) within the RPA by

$$\epsilon_{ij}(q,\omega) = \delta_{ij} - V_{ij}(q)\Pi_{jj}(q,\omega), \tag{1}$$

where q is the 1D wave vector in the x direction of free motion, ω is the mode frequency ($\hbar = 1$ throughout this paper), $V_{ij}(q)$ the Coulomb interaction in the 1D wire representation, and $\Pi_{jj}(q,\omega)$ the 1D noninteracting irreducible polarizability function for the jth ''component'' (i.e., the jth wire with $j=1,2$ corresponding to the two wires). In an ideal 1D electron system the Coulomb interaction $V(q)$ in the wave-vector space is logarithmically divergent, but in our realistic finite width quantum-wire model with the confinement width a we obtain the intrawire [interwire] Coulomb interaction matrix element $V(q)[U(q)]$ by taking the quantizing confinement potential to be of infinite square-well type,[16]

$$V(q) = V_{11}(q) = V_{22}(q) = \frac{2e^2}{\epsilon_b}f(q), \tag{2}$$

$$U(q) = V_{12}(q) = V_{21}(q) = \pm\frac{2e^2}{\epsilon_b}g(q), \tag{3}$$

where ϵ_b is the background high-frequency lattice dielectric constant, the $+$ $(-)$ sign in Eq. (3) refers to interaction between the same (opposite) types of charge in the two wires, (the two wires could in principle have electrons and holes, respectively, rather than being just all electrons or all holes in both wires), and $f(q)$, $g(q)$ are form factors associated with confinement matrix elements, which are given, for our infinite square-well confinement model, by

$$f(q) = \int_0^1 dx K_0(|qax|)h(x), \tag{4}$$

$$g(q) = \int_0^1 dx K_0(q\sqrt{(ax)^2+d^2})h(x), \tag{5}$$

for two wires parallel to each other aligned in the x-z plane. Here K_0 is the zeroth-order modified Bessel function of the second kind, and the function $h(x) = (1-x)[2+\cos(2\pi x)] + 3\sin(2\pi x)/(2\pi)$. If the two wires are parallel to each other aligned in the x-y plane the interwire Coulomb form factor becomes [with $f(q)$ remaining the same]

$$g(q) = \int_0^1 dx K_0[|q(ax+d)|]h(x). \tag{6}$$

As $q\to 0$, $f(q),g(q) \sim K_0(|qa|) + C$, where C is a constant (independent of d) for $f(q)$, but a function of the interwire spatial separation d for $g(q)$. Note that as $d\to 0$ $U(q)$ becomes $V(q)$, as it should, because the two wires are identical.

The irreducible 1D polarizability $\Pi_0(q,\omega)$ in the pure 1D system is given by the bare bubble diagram. The analytic form of $\Pi_{ii}^0(q,\omega)$ for complex frequency is given by[7]

$$\Pi_{ii}^0(q,\omega) = \frac{m_i}{\pi q}\ln\left[\frac{\omega^2 - (q^2/2m_i - qv_{Fi})^2}{\omega^2 - (q^2/2m_i + qv_{Fi})^2}\right], \tag{7}$$

where the principal value of logarithm (i.e., $-\pi < \text{Im}[\ln(z)] < \pi$) should be taken for complex frequency. In evaluating $\Pi_0(q,\omega)$ for real frequency, the usual retarded limit $\omega \to \omega + i0^+$ is implied. In Eq. (7) m_i and v_{Fi} are the effective band mass and the Fermi velocity, respectively. In the long-wavelength limit ($q\to 0$), we can expand the irreducible 1D polarizability as

$$\Pi_{ii}^0(q,\omega) \approx \frac{2v_{Fi}}{\pi}\frac{q^2}{\omega^2 - (qv_{Fi})^2}, \tag{8}$$

where $v_{Fi} = k_{Fi}/m_i$ is the Fermi velocity with a Fermi momentum $k_{Fi} = \pi n_i/2$ for the ith 1D component with n_i being the 1D density in the ith component. Since RPA is known to be valid in the long-wavelength limit ($q\to 0$), the limiting forms for the polarizability would be sufficient for our analytic calculations since we are interested in the leading-order wave-vector dependence of the collective modes of the sys-

tem. [For our numerical results we use the full 1D $\Pi(q,\omega)$ as given in Eq. (7).] Note that Π, v_F, k_F, etc., refer to the noninteracting or the bare 1D system, and are therefore perfectly well defined.

The expression for the 1D polarizability $\Pi_0(q,\omega)$ given in Eq. (7) assumes that the system is pure and free from any impurity scattering. In the presence of impurity scattering characterized by a level broadening or damping γ, the polarizability Π_γ can be evaluated by means of the standard perturbation theory[19] to include the impurity scattering induced vertex correction. The impurity scattering effects are introduced diagrammatically in the RPA by including impurity ladder diagrams into the electron-hole bubble consistently with self-energy corrections in the electron Green's function. Since the exact expression for $\Pi_\gamma(q,\omega)$ within this diagrammatic approach is complicated, we use in the numerical calculation a particle-conserving approximation for arbitrary values of q and ω, given by Mermin.[19] The Mermin expression is, in fact, equivalent to the diagrammatic result at long wavelength as long as the density of states renormalization by impurity scattering is negligible. In this relaxation-time approximation,[19] with the impurity scattering induced level broadening $\gamma=1/(2\tau)$, the polarizability is given by

$$\Pi_\gamma(q,\omega)=\frac{(\omega+i\gamma)\Pi_0(q,\omega+i\gamma)}{\omega+i\gamma[\Pi_0(q,\omega+i\gamma)/\Pi_0(q,0)]}. \qquad (9)$$

For small q and ω, the polarizability within the Mermin formula becomes

$$\Pi_\gamma(q,\omega)\approx\frac{nq^2}{m\omega(\omega+i\gamma)}. \qquad (10)$$

This approximate formula gives the same long-wavelength and low-frequency diffusive behavior as one gets from the diagrammatic approach.[15] In this paper, we take the impurity scattering induced broadening γ as a constant phenomenological parameter, which, for example, could be taken from the experimentally measured carrier mobility $\mu=e^2\tau/m$, with $\gamma=1/(2\tau)$.

The condition for the existence of a collective mode is given by the zeros of $|\epsilon|$, the determinant of the dielectric tensor defined by Eq. (1). For a two-component system without any tunneling, we have within RPA:

$$1-V(q)[\Pi_{11}^0(q,\omega)+\Pi_{22}^0(q,\omega)]$$
$$+[V(q)^2-U(q)^2]\Pi_{11}^0(q,\omega)\Pi_{22}^0(q,\omega)=0, \qquad (11)$$

with $i,j=1,2$ being the two charge components in confined wires 1 and 2. This equation indicates that the sign of the charge components forming the plasma has no effect on the dispersion relation of the collective modes of a two-component system.

The analytical formulas for the long-wavelength plasmon dispersion can be obtained even in the general situation where the two charge components have different Fermi wave vectors and Fermi energies (by virtue of having, for example, different effective masses $m_{1,2}$ and densities $n_{1,2}$). In this section we study the collective modes in this general situation (i.e., $d\neq0$, $n_1\neq n_2$, and $m_1\neq m_2$) although we should

emphasize that such a completely general situation is not physically particularly applicable (because in most existing quantum-wire systems either one has $m_1=m_2$ and $d\neq0$ or $m_1\neq m_2$ and $d=0$, corresponding, respectively, to a biwire system or an EHP system), and in Sec. IV, we investigate, in detail, the modes in a photoexcited homogeneous (i.e., $d=0$) 1D EHP ($d=0$, $n_1=n_2$, $m_1\neq m_2$) where the electrons and holes are not spatially separated, but have different effective masses.

First, we consider the plasmons of a symmetric two-component system having equal densities ($n_1=n_2=n$), masses ($m_1=m_2=m$), and a finite interwire separation d, and neglecting impurity scattering effects ($\gamma=0$) for simplicity. In this case $\Pi_{11}^0=\Pi_{22}^0$ and Eq. (11) becomes

$$[1-2V_+(q)\Pi_{11}^0(q,\omega)]\times[1-2V_-(q)\Pi_{11}^0(q,\omega)]=0, \qquad (12)$$

where $V_\pm=[V(q)\pm U(q)]/2$. By solving Eq. (12) we have two branches of collective modes corresponding to the in-phase OP mode ω_+ and the out-of-phase AP mode ω_- (the in-phase ω_+ and out-of-phase ω_- nomenclature applies to the situation when both components are electrons or both are holes; otherwise, i.e., for an electron-hole system, ω_+ is the out-of-phase mode and ω_- the in-phase mode):

$$\omega_\pm^2(q)=\frac{A_\pm(q)[v_Fq+E(q)]^2-[v_Fq-E(q)]^2}{A_\pm(q)-1}, \qquad (13)$$

where $E(q)=q^2/2m$ and $A_\pm(q)=\exp[\pi q/(2mV_\pm)]$. The optical mode ω_+ (acoustic mode ω_-) indicates the symmetric in-phase (antisymmetric out-of-phase) density oscillation of the coupled system assuming the two carriers have the same charge. In the long-wavelength limit $q\to0$, Eq. (13) becomes

$$\omega_\pm(q\to0)=q\left[v_F^2+\frac{4}{\pi}v_FV_\pm(q\to0)\right]^{1/2}, \qquad (14)$$

where the asymptotic forms of the Coulomb potential $V_\pm(q)$ as $q\to0$ are given by

$$V_+(q\to0)=\frac{2e^2}{\epsilon_b}[K_0(|qa|)+1.97269\cdots],$$

$$V_-(q\to0)=\frac{2e^2}{\epsilon_b}\int_0^1dx\ln\left[\frac{y(x)}{x}\right]$$
$$\times\left[(1-x)[2+\cos(2\pi x)]+\frac{3}{2\pi}\sin(2\pi x)\right], \qquad (15)$$

where $y(x)=[x^2+(d/a)^2]^{1/2}$ $[y(x)=x+d/a]$ for the system aligned in the x-z (x-y) plane. As $q\to0$, $V_+(q)$ diverge as $-\ln(qa)$, but the leading-order term in $V_-(q)$ is finite and depends only on the spatial separation d. Therefore the leading-order term in the 1D OP dispersion $\omega_+(q)$ is enhanced by a factor $\sqrt{2}$ compared to the one-component system (corresponding trivially to the change in density from n to $2n$) and behaves as $q|\ln(qa)|^{1/2}$ as $q\to0$. The dispersion of the acoustic mode $\omega_-(q)$ shows a purely linear behavior $\omega_-(q)=v_-q$ for $q\to0$ with the velocity $v_-=v_F[1+4V_-(q=0)/(\pi v_F)]^{1/2}$ as $q\to0$, and lies always above the
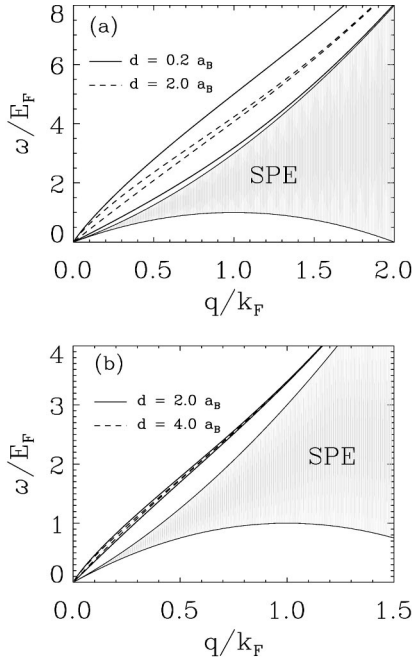
FIG. 1. Calculated RPA collective-mode dispersion for different spatial separations between the two identical quantum wires; (a) $n_1=n_2=0.6\times10^6$ cm^{-1} and (b) $n_1=n_2=10^6$ cm^{-1}. Here the higher (lower) frequency mode corresponds to the OP (AP) mode in each case. Shaded region indicates the single-particle excitation (SPE) continuum.

single-particle Landau damping region because $v_->v_F$. The spatial separation of the two wires produces a weak second-order correction to the OP dispersion in the two-component system. For $d=0$, the ω_- mode becomes degenerate with the electron-hole continuum (i.e., $v_-=v_F$) in the long-wavelength limit, and the ω_+ mode becomes that of the corresponding one-component system with a total density $N=2n$. As the spatial separation increases the optical (acoustic) plasmon mode frequency decreases (increases) slowly at long wavelengths. For the system with an infinite separation, the two modes become uncoupled, and have the same dispersion as the 1D plasmon in the one-component system with a total density n.

In Fig. 1 we show our calculated collective-modes dispersion for different spatial separations between the two identical quantum wires; (a) $d=0.2a_B$ and $2.0a_B$ with $n=0.6\times10^6$ cm^{-1}, and (b) $d=2.0a_B$ and $4.0a_B$ with $n=10^6$ cm^{-1}, where $a_B(\approx100$ Å$)$ is the Bohr radius of the GaAs system and we use this as our length unit throughout this paper. In Fig. 1 we use the parameters $m=0.067m_0$ and the wire width $a=a_B$. As discussed above, we find that the plasmon dispersion strongly depends on the interwire Coulomb correlation determined by d. In these figures we find that for larger spatial separation the energy difference of $\omega_\pm$ modes is small because as d increases the interwire Coulomb correlation decreases. The important point to note is that both the $\omega_\pm$ modes remain undamped upto very large wave vectors due to the suppression of 1D SPE, and therefore experimental observation of $\omega_\pm$ charge-density modes in coupled biwire systems should be relatively easy via light scattering or far-infrared spectroscopy.

Now we consider the collective-mode spectrum in a gen-

eral system where the two components may have different densities and masses. The general situation with $d=0$ is of special experimental relevance because it describes the photoexcited 1D EHP system — we therefore defer the discussion of the $d=0$ 1D EHP system to Sec. IV. Since there is a low-energy gap in the 1D SPE, we look for undamped plasmons in two regions: the high-frequency region ($\omega>qv_{F1}$, qv_{F2}) and the low-frequency region ($qv_{F1}>\omega>qv_{F2}$). (We choose $v_{F1}>v_{F2}$ throughout this section without any loss of generality.) In the long-wavelength limit ($q\to0$), we solve Eq. (11) using Eq. (8) to get

$$\omega_+(q)=qv_{F1}\left[1+\frac{2(1+\alpha)}{\pi v_{F1}}V_1(q\to0)\right]^{1/2}, \quad (16)$$

$$\omega_-(q)=qv_{F1}\left[\alpha+\frac{8}{\pi v_{F1}}\frac{\alpha}{1+\alpha}V_-(q\to0)\right]^{1/2}, \quad (17)$$

where $\alpha=v_{F2}/v_{F1}=(n_2/n_1)(m_1/m_2)\le1$. In the long-wavelength limit, these asymptotic expressions for $\omega_\pm$ are valid in both the high-frequency ($\omega>qv_{F1}$) and the low-frequency ($qv_{Fl}>\omega>qv_{F2}$) regimes. The condition for the existence of an undamped AP mode (ω_-) in the high-frequency regime ($\omega>qv_{F1}$) is given by $v_-(\alpha,d)>v_{F1}$, or

$$\alpha+\frac{8}{\pi v_{F1}}\frac{\alpha}{1+\alpha}V_-(q\to0)>1. \quad (18)$$

We find that the condition defined by the inequality [Eq. (18)] leads to the conclusion that within RPA ω_- can exist as an undamped mode either for a large spatial separation (and arbitrary α) or for almost equal Fermi velocities, i.e., $\alpha\approx1$, (and arbitrary d). As α decreases the system should have a large spatial separation to have an undamped high-energy AP mode. For $\alpha=1$ (e.g., equal mass and density), we find that the acoustic mode lies in the high-frequency regime and is always undamped for arbitrary d. This is also true in 2D bilayer systems with finite layer separations, where the AP mode is undamped as long as $\alpha=1$ and $d\neq0$. The condition for the existence of the AP mode in the low-frequency regime ($qv_{F1}>\omega_->qv_{F2}$) is given by $v_{F2}<v_-(\alpha,d)<v_{F1}$. Due to the energy gap in the 1D SPE the AP mode is undamped in this regime. The existence of the undamped AP mode in the low-frequency regime for arbitrary α and d is a unique phenomenon in the 1D two-component system arising entirely from the nonexistence of low-energy SPE in 1D. In 2D or 3D two-component system the low-frequency regime is necessarily accompanied by Landau damping due to the presence of the low-energy SPE continua.

In Fig. 2 we show our numerically calculated longitudinal collective modes (for different d and α) with a fixed density $n_1=0.6\times10^6$ cm^{-1}, effective mass $m_1=0.067m_e$ (corresponding to the effective electron mass of the GaAs), and a wire confinement $a=a_B$. In these figures the higher- (lower-) energy mode ω_+ (ω_-) denotes the optical (acoustic) mode. In Fig. 2(a) we use these parameters: the spatial separation of the two wires $d=0.5a_B$ and $\alpha=(n_2/n_1)(m_1/m_2)=0.6$. (Note that α determines the density of the component two for a given n_1 and m_1, m_2. For example, if $m_2=m_1$ we have $n_2=0.6n_1$.) With these param-
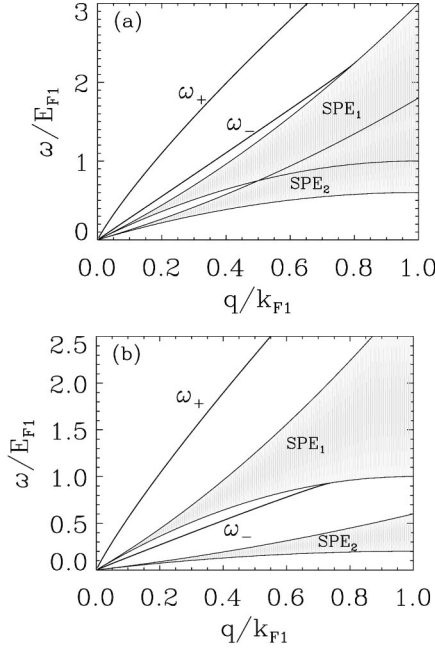
FIG. 2. Calculated RPA collective mode dispersion (a) for the spatial separation $d=0.5a_B$ and $\alpha=v_{F2}/v_{F1}=0.6$; and (b) for $d=0.2a_B$ and $\alpha=0.2$. The ω_+ (ω_-) lines denote the OP (AP) mode and SPE_1 (SPE_2) denote the single-particle excitation of the component 1 (2).

eters the velocity of the acoustic mode v_- exceeds the Fermi velocity of the component one ($v_->v_{F1}$) and lies well above the SPE's of both components (high-frequency regime). In Fig. 2(b) we choose the parameters which limit the v_- between v_{F1} and v_{F2}: $d=0.2a_B$ and $\alpha=0.2$. (Note that this requirement restricts d to unrealistically small values.) Thus the undamped AP mode with these conditions lies in the low-frequency regime ($v_{F2}<v_-<v_{F1}$) which corresponds to the regime between two SPE's. The important point is that in both cases (''large'' d and α, and ''small'' d and α) the AP is undamped in 1D in contrast to higher dimensional systems.

Next we investigate the plasmon modes of the two-component system in the presence of impurity scattering. We calculate the plasmon dispersion of a spatially separated 1D two-component system with equal masses and densities ($\alpha=1$) in the presence of impurity scattering (characterized by a constant level broadening γ). With the approximation for the polarizability function for small q and ω defined by Eq. (10) the plasmon dispersion is given by

$$\omega_\pm(q) \sim -i\frac{\gamma}{2} + \sqrt{-\frac{\gamma^2}{4} + \frac{2nq^2}{m}V_\pm(q)}, \quad (19)$$

where ω_+ (ω_-) indicates the OP (AP) mode. Note that for $\gamma \to 0$, Eq. (19) recovers the result previously obtained for the pure two-component system. Thus in the presence of impurity scattering the plasmon modes acquire a wave-vector dependent imaginary part which corresponds to a plasma damping, $\omega_\pm(q)=\omega_{p\pm}(q)-i\alpha_\pm(q)$. The plasmon becomes overdamped at small q as it becomes completely imaginary for small q, i.e., the plasmon modes are totally overdamped below the critical wave vectors $q_{c\pm}$ and exist
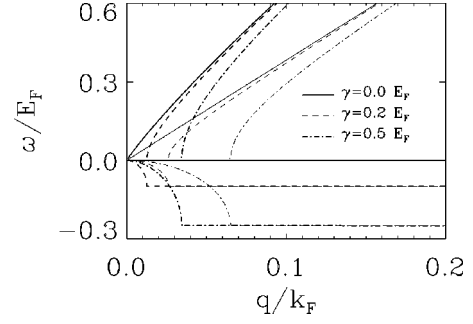

FIG. 3. RPA plasmon dispersions of the 1D two-component system are shown for various impurity scattering rates γ as given in the figure. Here $\omega>0$ gives the dispersions of the mode and $\omega<0$ the dampings of the mode. Thick (thin) lines correspond to the OP (AP) mode. The overdampings of the plasmons for $q<q_{c\pm}$ are clearly seen. We use the parameters: $\alpha=1$ ($n_1=n_2=0.6 \times 10^6$ cm^{-1} and $m_1=m_2=0.067m_e$) $a=a_B$, and $d=0.5a_B$.

only for wave vectors q larger than these critical values. (Note that the plasmon broadening $\alpha_\pm(q)$ is, in general, determined by the imaginary part of the complex plasmon mode, and is different from the level broadening γ.) For $q>q_{c\pm}$ the plasma dampings are roughly comparable to the half of the impurity scattering, i.e., $\alpha_\pm(q) \approx \gamma/2$. From Eq. (19) we find the critical wave vectors (below which the plasmon is no longer a well-defined collective mode) as

$$q_{c+} = \frac{K}{\sqrt{2}|\ln(Ka/\sqrt{2})|},$$

$$q_{c-} = \frac{K}{\sqrt{\dfrac{\epsilon_b}{2e^2}V_-(q=0)}}, \quad (20)$$

where $K=\gamma\sqrt{m\epsilon_b/(8ne^2)}$. As the impurity scattering rate γ increases the critical wave vectors $q_{c\pm}$ also increase. The q_{c+} (just as ω_+ itself) depends weakly on d, but q_{c-} (just as ω_-) is strongly affected by d. As $d \to 0$ the intra- and inter-wire Coulomb interactions become the same, $V_-(q) \to 0$, and consequently $q_{c-} \to \infty$. Thus, for the system with a large impurity scattering and a small spatial separation we have only the OP mode in the long-wavelength limit. In general, we have $q_{c-}>q_{c+}$ from Eq. (20), which means that the AP mode is easily affected by impurity scattering (and is therefore more difficult to observe experimentally.)

In Fig. 3 we show the plasmon dispersion calculated numerically by using the full polarizability, Eq. (9), in the presence of finite impurity scattering. We find zeros of the complex dielectric function of the 1D two-component system in the presence of impurity scattering, i.e., $\epsilon(q,\omega)=0$, to obtain the plasmon dispersion curves. In Fig. 3 the curves with $\omega>0$ give the plasma frequency or the real part $[\omega_p(q)]$, and those with $\omega<0$ give the plasma damping or the imaginary part (α) of the complex zero solutions $[\omega(q)]$. The figure shows that the plasmons are overdamped below critical wave vectors $q<q_{c\pm}$. The critical wave vectors, $q_{c\pm}$, below which the plasmon does not exist due to impurity scattering effects, depend on the density and the impurity

scattering rate. We note that the overdamping of the plasmon mode occurring for small q is a direct consequence of the diffusive nature of the electron dynamics. We emphasize that this long-wavelength impurity scattering induced suppression of collective modes is more severe in 1D than in 2D or 3D (in 3D, because the OP is gapped, it is hardly affected by impurity scattering.)

Finally, we study the dynamical structure factor, $S(q,\omega)$ $\propto \text{Im}[\epsilon(q,\omega)^{-1}]$, which gives a direct measure of the oscillator strength of the density fluctuation spectrum, and many experimental probes such as inelastic electron and Raman scattering spectroscopies are directly related to the dynamical structure factor.[20] Equivalently, the dynamical structure factor is a measure of the spectral weight carried by the particular collective mode of the electron liquid. An undamped plasmon shows up as a δ-function peak in $S(q,\omega)$ indicating the existence of a simple zero of $\epsilon(q,\omega)$. When both $\text{Re}[\epsilon]$ and $\text{Im}[\epsilon]$ become zero [i.e., $\epsilon(q,\omega)=0$] the imaginary part of the inverse dielectric function $\text{Im}[\epsilon(q,\omega)^{-1}]$ is a δ function with the strength

$$W(q) = \frac{\pi}{|\partial \text{Re}[\epsilon(q,\omega)]/\partial\omega|_{\omega=\omega_\pm(q)}}, \quad (21)$$

where $\omega_\pm(q)$ are the plasmon dispersions for the system. The damped plasmon ($\alpha \neq 0$), however, corresponds to a broadened peak in $S(q,\omega)$—for larger broadening, as for $q < q_c$ in the system with impurity scattering, the plasmon is overdamped and there is no peak in $S(q,\omega)$. At long wavelengths ($q\to 0$), the optical plasmon ω_+ mostly exhausts the f-sum rule and carries almost all the spectral weight. $W(q)$ approaches zero as $q\to 0$ because the 1D plasma frequency vanishes. Note that the small weight of the AP mode at long wavelengths makes it particularly susceptible to collisional damping effects in 1D two-component system. For the system with the same effective mass and a large spatial separation, the acoustic plasmon mode has an energy comparable to that of the optical plasmon mode, which gives the enhanced spectral weight associated with the AP mode.

In Fig. 4 the $\text{Im}[\epsilon(q,\omega)^{-1}]$ is plotted for different wave vectors as a function of the frequency for two different systems. In Fig. 4(a) we choose the parameters such that the AP mode lies in the low-frequency regime: $n_1 = 1.0 \times 10^6$ cm^{-1}, $a=2a_B$, $\alpha=0.2$, and $d=0.5a_B$. In Fig. 4(b) we choose the parameters such that the AP mode lies in the high-frequency regime: $n_1 = 0.6 \times 10^6$ cm^{-1}, $a=a_B$, $\alpha =0.9$, and $d=a_B$. The insets in Fig. 4 show the weight $W(q)$ of the plasmon modes. For pure system the plasmon peaks become δ-function peaks with weights given in the inset, but with impurity scattering rate $\gamma_1 = 0.1E_{f1}$ and $\gamma_2 =0.1E_{f2}$, we show broadened peaks giving the damped plasmon modes. As shown in Fig. 4 the spectral weight of the acoustic mode is comparable with that of the optical mode at finite wave vectors, but not in the long-wavelength limit. With the enhanced spectral weight the acoustic plasmon mode in 1D should be more easily observable than in higher dimensions and may significantly affect physical properties of the quasi-1D two-component systems. The results presented in this section indicate that the AP mode should be observable in double wire structures under experimentally realizable conditions.
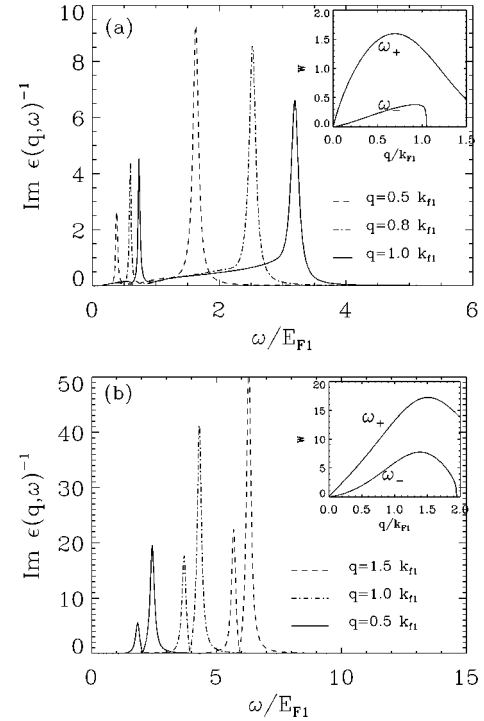

FIG. 4. The RPA dynamical structure factor $\text{Im}[\epsilon(q,\omega)^{-1}]$ in 1D two-component systems as a function of frequency ω for different wave vectors q. We use the parameters: (a) $n_1 = 10^6$ cm^{-1}, $a=2a_B$, $\alpha=0.2$, and $d=0$, (b) for $n_1=0.6\times 10^6$ cm^{-1}, $a=a_B$, $\alpha=0.9$, and $d=a_B$. We use the impurity scattering rate $\gamma_1 =0.1E_{F1}$ and $\gamma_2=0.1E_{F2}$ in both figures. The inset shows the weights $W(q)$ of the plasmon modes in the absence of the impurity scattering.

III. BIWIRE WITH WEAK TUNNELING

In this section we analytically calculate the collective mode dispersions in biwire structures ($\alpha=1$, i.e., $n_1=n_2$ and $m_1=m_2$, and $d\neq 0$) *in the presence of significant interwire quantum tunneling*, all earlier work in the previous section having dealt with the zero tunneling limit. Since our focus is on understanding tunneling effects in this section, we put $\alpha =1$ with no loss of generality. In the presence of interwire tunneling, the electron energy eigenstates $E_\pm$ should be used[21] as the basis set rather than the wire index which is no longer a good quantum number. The energy levels $E_\pm =\epsilon(k)\pm t$, where $\epsilon(k)=k^2/2m$ is the parabolic one-electron 1D kinetic energy in each wire and t is the tunneling strength, are the usual symmetric and antisymmetric one-electron eigenstates in the presence of tunneling with the single-particle symmetric-antisymmetric (SAS) gap given by $\Delta_{SAS}=E_+ - E_- =2t$. In the SAS representation the collective-mode spectra become decoupled by virtue of the symmetric nature of our biwire system (i.e., both wires identical with equal electron density), and the collective density-fluctuation spectra are given by the following two equations for the in-phase and the out-phase plasmon modes $\omega_\pm$, respectively:

$$\epsilon_+(q,\omega)=1-V_+(q)[\Pi_{++}(q,\omega)+\Pi_{--}(q,\omega)]=0, \quad (22)$$

and

$$\epsilon_-(q,\omega)=1-V_-(q)[\Pi_{+-}(q,\omega)+\Pi_{-+}(q,\omega)]=0, \tag{23}$$

where $V_\pm(q)=V(q)\pm U(q)$ with $V(q)$ and $U(q)$ being, respectively, the intrawire and interwire Coulomb interaction matrix elements given in Eqs. (2) and (3). The $\Pi_{\alpha\beta}(q,\omega)$ in Eqs. (22) and (23), with $(\alpha,\beta)=(+,-)$, are the noninteracting SAS polarizability functions within our RPA theory:

$$\Pi_{\alpha\beta}(q,\omega)=2\int\frac{dk}{(2\pi)}\frac{f_\alpha(\mathbf{k}+\mathbf{q})-f_\beta(\mathbf{k})}{w+E_\alpha(\mathbf{k}+\mathbf{q})-E_\beta(\mathbf{k})}, \tag{24}$$

where $f_{\alpha,\beta}$ are Fermi occupancy factors.

Solving Eqs. (22)–(24) we obtain the collective density-fluctuation spectra of the coupled biwire system. In the absence of tunneling, $t=0$, one has $E_+=E_-=\varepsilon(\mathbf{k})$, and one then recovers in a straightforward fashion the results we have in Sec. II, i.e., the in-phase optical $[\omega_+\sim q|\ln(qa)|^{1/2}]$ and the out-of-phase acoustic ($\omega_-\sim q$) plasmons of a biwire system without any electron tunneling. It is, in fact, straightforward to obtain analytically [from Eqs. (22)–(24)] the long-wavelength ($q\rightarrow 0$) plasma modes of the coupled biwire system *including effects of interwire tunneling*. We obtain in the long-wavelength limit the following results:

$$\omega_+^2(q\rightarrow 0)=q^2\left[v_F^2+\frac{2}{\pi}(b_++b_-)v_F V_+(q)\right], \tag{25}$$

$$\omega_-^2(q\rightarrow 0)=\Delta_{SAS}^2+\frac{4k_F}{\pi}(b_+-b_-)V_-(q=0)\Delta_{SAS}, \tag{26}$$

where $v_F=k_F/m$ is the Fermi velocity and $b_\pm=(1\pm t/E_F)^{1/2}$ for $n>n_c=4m\Delta_{SAS}/\pi^2$ when both symmetric and antisymmetric levels are occupied (i.e., the 1D Fermi energy $E_F>\Delta_{SAS}$), and $b_+=2,b_-=0$ for $n\leq n_c$ when only the symmetric level is occupied (i.e., $E_F<\Delta_{SAS}$).

The most important qualitative feature of the plasmon dispersion in the presence of interwire tunneling is that even though the in-phase OP mode (ω_+) depends weakly on tunneling, the out-of-phase mode (ω_-), which is purely acoustic in the absence of tunneling ($\omega_-\sim q$ if $\Delta_{SAS}=0$), develops a plasmon gap at $q=0$ in the presence of nonzero tunneling. The plasmon gap $\Delta\equiv\omega_-(q=0)$ depends nontrivially on the 1D electron density n, the interwire tunneling amplitude t, and the interwire distance d. It is easy to see from Eq. (26) that this plasmon gap Δ, has the following behavior:

$$\Delta\sim\Delta_{SAS}\quad\text{or}\quad\sqrt{\Delta_{SAS}}, \tag{27}$$

depending on whether the interwire tunneling is strong or weak. It should be emphasized that the strikingly nonintuitive $\Delta_{SAS}^{1/2}$ dependence of the collective-mode gap (on the square root of the single-particle gap) is purely a Coulomb interaction effect, which dominates the collective excitation spectra in the weak tunneling situation. We mention the curious phenomenon that interwire tunneling converts the ω_- mode into an effective optical mode by opening up a long-wavelength plasmon gap (for $t=0$ the ω_- mode is the AP mode).

IV. PHOTOEXCITED ONE-DIMENSIONAL ELECTRON-HOLE PLASMA

In Secs. II and III we discussed a double wire system where the two one-dimensional charged components are separated by a distance d. Now we consider the possibility of acoustic plasmons in a photoexcited homogeneous (i.e., $d=0$) 1D EHP where the electrons and holes are not spatially separated. This is, in fact, the original context[10] in which the AP mode was first discussed in the solid-state plasma more than forty years ago. The photoexcited EHP in semiconductors is also the system in which most of the early investigations[11] of acoustic plasmons were carried out. Our reason for singling out the 1D EHP for a detailed investigation in this section (in principle, it is just the $d=0$ limit of Sec. II) is the existence of 1D EHP in real samples[22] from several groups where a search for 1D $\omega_\pm$ modes via light-scattering spectroscopy should be successful.

It has been known for a long time[10] that a two-component EHP allows for the existence of two collective modes, one of which (the low-frequency one) is linear in wave vector or acoustic at long wavelengths, and the other mode (the high-frequency or the optical plasmon) is essentially the combined collective charge-density oscillation of the whole system being therefore qualitatively similar to the usual plasmon mode in a single-component plasma. In an electron-hole two-component plasma, as appropriate in a photoexcited semiconductor system, the AP corresponds to the in-phase collective density-fluctuation excitation of electrons and holes, and the OP corresponds to their out-of-phase motion with respect to each other. [If the two components are both electrons or both holes, for example, in a biwire (as considered in Sec. II of the paper) or bilayer or a two-band system, then the AP signifies the out-of-phase collective mode and the OP the in-phase motion—in general, the acoustic mode is the neutral mode at long wavelengths and the optical mode the charged mode.] In spite of compelling theoretical arguments[10,23,24] for the existence of ''quantum'' AP in degenerate two-component homogeneous electron-hole solid-state plasmas the experimental observation of low-temperature AP in two- and three-dimensional homogeneous electron-hole semiconductor plasmas has been very severely hindered by Landau damping effects. It turns out that in two- and three-dimensional degenerate homogeneous EHP the AP is necessarily Landau damped (by decaying into single-particle excitations) and is in fact unobservable as a well-defined mode unless the effective-mass ratio between the two species is extremely large.[10,23,24] This has prevented an unambiguous observation[11] of a quantum AP in degenerate solid-state EHP although the corresponding classical AP (in the nondegenerate high-temperature electron-ion plasma) was experimentally observed[25] almost forty years ago.

In this section we show that the elusive quantum AP in the homogeneous (i.e., $d=0$) EHP should be relatively easy to observe in the degenerate 1D EHP (Ref. 22) confined in semiconductor quantum-wire structures due to the severe suppression of single-particle excitations in one-dimensional
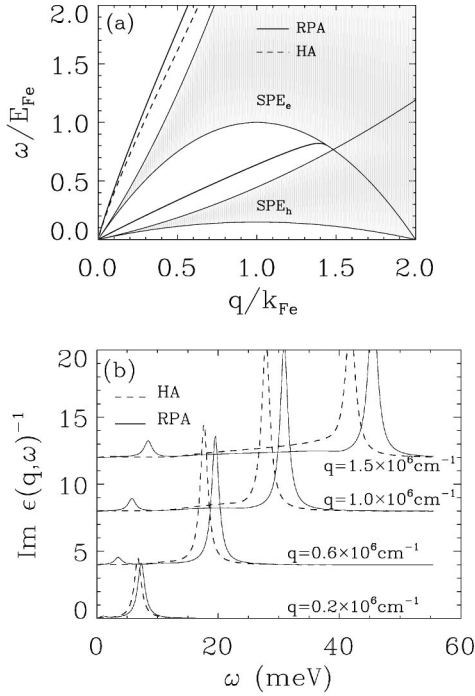
FIG. 5. The calculated (a) plasmon dispersions and (b) spectral weights for densities $n_e = n_h = 1.0 \times 10^6$ cm^{-1} in the photoexcited GaAs quantum-wire EHP within both RPA (solid lines) and HA (dashed lines). The SPE$_{e,h}$ denote the single-particle excitation of the electron and the hole, respectively. At this density the AP mode ω_- is completely suppressed by the local-field effects in the HA (no dashed line corresponding to the AP mode exists within HA).

systems. In particular, within the RPA which should be quantitatively valid in one dimension by virtue of the smallness of vertex corrections, the AP mode in a 1D EHP in GaAs quantum wires should be *completely* undamped up to a rather large wave vector $q \gtrsim k_F$, in contrast to two-/three-dimensional EHP where the AP is damped in GaAs and is essentially unobservable. We believe that resonant inelastic light-scattering spectroscopy, which has already been successfully used[6] in observing the 1D plasmon in *single-component* (*n*-doped) GaAs quantum wires, is the ideal tool in the search for the AP in *photoexcited* (undoped) two-component EHP in GaAs quantum wires. Theoretical results presented in this section show that the 1D in-phase AP mode should be readily experimentally observable in resonant inelastic light-scattering experiments performed on photoexcited 1D EHP (Ref. 22) in narrow GaAs-AlGaAs quantum wires.

We put $d = 0$ in the formalism developed in Sec. II of the paper and allow for the possibility of different masses m_e and m_h taking equal densities $n_e = n_h = n$ of the electrons and holes. Below we present and discuss our results for collective modes in 1D EHP both in the RPA and in the Hubbard approximation (HA) where one includes a local-field correction to the RPA noninteracting polarizability. The inclusion of local-field corrections (HA) beyond RPA distinguishes this section from Sec. II where strict RPA was used — our motivation for using HA (as well as RPA) is to make our results more realistic for the experimental systems where local-field corrections may very well be important at the experimentally feasible densities and wave vectors. The dy-
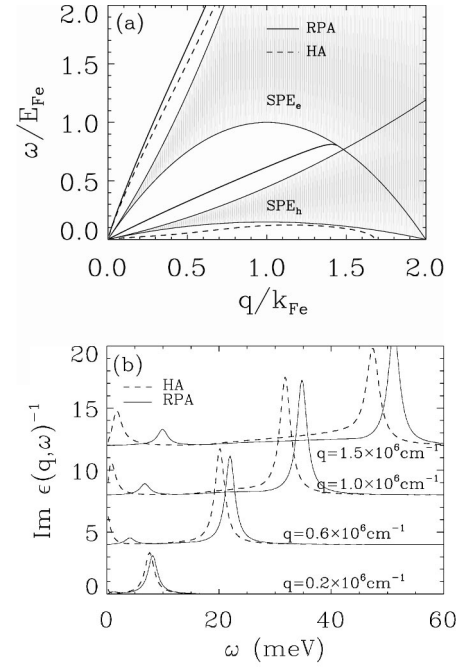

FIG. 6. The same as Fig. 5 for densities $n_e = n_h = 1.2 \times 10^6$ cm^{-1}. Note that the AP mode ω_- lies below the SPE$_h$ due to the local-field effects.

namical dielectric function in the HA is given by

$$\epsilon_H(q,\omega) = \{1 - V(q)[1 - G_e(q)]\Pi_e^0(q,\omega)\}$$
$$\times \{1 - V(q)[1 - G_h(q)]\Pi_h^0(q,\omega)\}$$
$$- V(q)^2 \Pi_e^0(q,\omega)\Pi_h^0(q,\omega), \quad (28)$$

where $G_{e,h}(q)$ is a simple static local-field correction to the RPA and is given by $G_{e,h}(q) = V(\sqrt{q^2 + k_{Fe,h}^2})/2V(q)$, where $k_{Fe,h}$ are the Fermi wave vector of the electron and hole, respectively. The calculation in the HA is similar to that in the RPA with the RPA dielectric function [Eq. (1)] being replaced by the HA dielectric function [Eq. (28)]. By putting $d = 0$ we have $V_-(q) = 0$, $V_+(q) = V(q)$. Thus in the long-wavelength limit $q \to 0$, we have the plasmon mode dispersions within RPA from Eqs. (16) and (17):

$$\omega_+(q) = q v_{Fe} \left[1 + \frac{2(1+\alpha)}{\pi v_{Fe}} V(q \to 0) \right]^{1/2}, \quad (29)$$

$$\omega_-(q) = \sqrt{\alpha} q v_{Fe}, \quad (30)$$

where $\alpha \equiv v_{Fh}/v_{Fe}$ corresponds to the mass ratio m_e/m_h since $n_e = n_h$. As the mass ratio decreases ($\alpha \to 0$), the OP mode (ω_+) becomes the plasmon mode of the one-component system. Since $0 < \alpha < 1$ we have $q v_{Fh} < \omega_-(q) < q v_{Fe}$. The AP mode within RPA lies always in the undamped region (low-frequency regime) between two SPE's. This undamped 1D AP mode ω_- in the long-wavelength limit is fundamentally different from the AP mode of the higher dimensional EHP since the presence of the low-energy Landau damping region in 2D or 3D gives rise to the complete damping of AP mode, unless α is very small — in the 1D EHP the AP mode is undamped within RPA for arbitrary values of α ($\alpha < 1$ by choice).
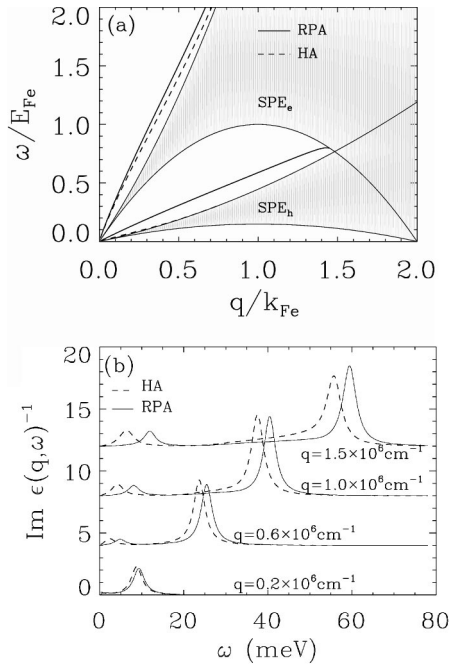
FIG. 7. The same as Fig. 5 for densities $n_e = n_h = 1.5 \times 10^6$ cm^{-1}. Note that the AP mode ω_- lies between SPE$_e$ and SPE$_h$.

In Figs. 5–7 we show the numerically calculated plasmon modes and spectral weights for different densities in the photoexcited GaAs quantum-wire 1D EHP within both RPA and HA. In Figs. 5–7 we use the parameters corresponding to GaAs: $m_e = 0.067m_0$, $m_h = 0.45m_0$, $\epsilon_b = 11$, and the confinement width of the wire $a = a_B$. We also use a level broadening $\gamma_{e,h} = 0.1E_{Fe,h}$ due to the impurity scattering in calculating the mode spectral weights. Note that in the long-wavelength limit the RPA AP modes are undamped (except, of course, for impurity damping) for all densities because of the absence of long-wavelength Landau damping. In general, similar to the corresponding higher dimensional situations the local-field effects in the HA reduce the plasma frequencies[15] compared with the RPA results, in particular, in the low-density system. Since the ω_+ mode exhausts the f-sum rule in the long-wavelength limit, the local-field correction has relatively little effect on the ω_+ mode. The ω_- AP mode is, however, very strongly affected by local-field effects. Figure 5 shows the results for the EHP density $n_e = n_h = 10^6$ cm^{-1}: At this density we find the remarkable result that the ω_- AP mode is completely suppressed by local-field effects as it gets pushed into the SPE Landau damping continua. Thus in Fig. 5(a) the AP mode dispersion within HA does not show up because ω_- lies completely in the Landau damping continuum. Figure 5(b) shows that within RPA (solid lines) the ω_- mode (low-energy peaks) carries an appreciable spectral weight which is comparable to that carried by the OP mode ω_+ (high-energy peaks), however, within HA (dashed lines) the ω_+ mode actually carries all the spectral weight (we find only the high-energy ω_+ peaks in the HA with the low-energy ω_- peaks being completely suppressed). As density increases the (completely suppressed) ω_- mode in HA reappears in the low-energy regime as the AP mode comes out of the Landau continuum. In Figs. 6 and 7 we show the results for density $n_e = n_h$

$= 1.2 \times 10^6$ cm^{-1} and $n_e = n_h = 1.5 \times 10^6$ cm^{-1}, respectively. At the density $n_e = n_h = 1.2 \times 10^6$ cm^{-1} the ω_- mode reappears below the SPE$_h$ in the HA. This ω_- mode lying below SPE$_h$ is undamped due to the low-energy SPE gap in 1D and is a characteristic feature of 1D EHP. The spectral weight of the undamped ω_- mode in the low-energy region (at higher density) is comparable to that of the ω_+ mode even within HA [Fig. 6(b)]. At very high density (Fig. 7) $n_e = n_h = 1.5 \times 10^6$ cm^{-1} the local-field corrections are weak, and we find that the ω_- mode (in the HA) lies between SPE$_e$ and SPE$_h$ and is undamped in the long-wavelength limit. The calculated spectral weight in the HA is comparable to that in the RPA in these high-density systems. One conclusion of our HA-based calculations is that one should use higher EHP densities for an unambiguous observation of undamped 1D AP — this is consistent with our RPA results also, where Landau damping is absent, because in RPA higher carrier densities imply quantitatively weaker effects of impurity level broadening.

Given the unique nature of the SPE continua (and the strong low-energy suppression of Landau damping) in the 1D system, the question naturally arises about whether the collective-mode behavior in 1D EHP is fundamentally different from that in 2D and 3D systems, where the AP mode is usually unobservable due to its unavoidable decay via Landau damping to the electron (i.e., the lighter-mass component) SPE unless α is very small (i.e., the mass ratio very small, $m_e \ll m_h$) which cause the Landau damping to be small, but still nonzero. In the 1D EHP, however, there are three (as opposed to only one in 2D and 3D EHP) Landau damping-free regimes in the ω-q space — these are [see Figs. 5(a), 6(a), or 7(a)] the high-energy–low wave-vector regime above the lighter-mass SPE continuum (which is present in 2D and 3D systems also), the low-energy regime below both the SPE continua, and the intermediate energy — low to intermediate wave-vector regime in the SPE gap between the SPE continua of the two components (we emphasize that Landau damping of collective modes is allowed in 2D and 3D systems in the last two regimes even in the RPA because there is no low-energy gap in the SPE continuum in higher dimensions). To emphasize the qualitative difference between 1D EHP and its higher dimensional counterparts with respect to the Landau damping characteristics of the collective modes, we provide in Figs. 8 and 9 our calculated RPA results for collective-mode dispersion and damping in 2D and 3D EHP, respectively, choosing the same effective mass, lattice dielectric constant, level broadening, and ''approximately equivalent'' carrier densities. One can see that in Figs. 8(a), the 2D EHP case, and 9(a), the 3D EHP case, the OP mode is above the SPE continua of both components (exactly the same as in Figs. 5 –7 for the OP in 1D EHP) and is therefore not Landau damped whereas the AP mode in both case lies within the electron (i.e., the lighter-mass) SPE continuum (but above the hole SPE) and is therefore Landau damped by decaying into the quasiparticles of the electron component in the EHP. The contrast between the RPA results for the 2D/3D AP mode (Figs. 8 and 9) and the 1D AP mode (Figs. 5–7) is striking in terms of Landau damping — the 2D/3D AP mode is invariably Landau damped by being inside the SPE continuum of the lighter carrier component (i.e., the higher Fermi velocity v_{Fe}, in our case) where the
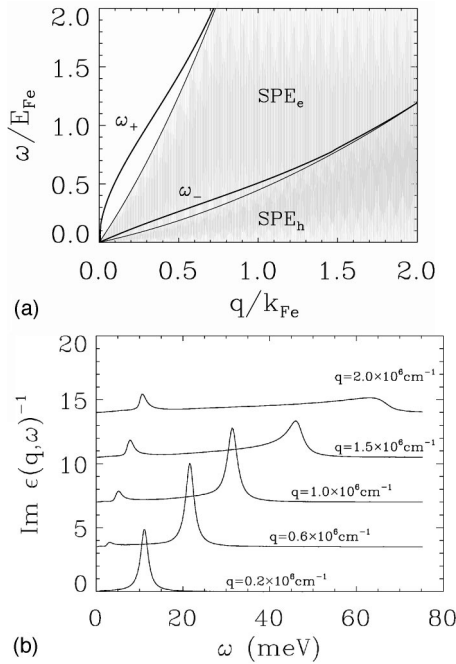
FIG. 8. The calculated (a) plasmon dispersions and (b) spectral weights for densities $n_e = n_h = 0.6 \times 10^{12}$ cm^{-2} in the photoexcited GaAs 2D EHP within RPA.

1D AP mode (within RPA) is undamped by being in the intermediate regime in between (the SPE ''gap'' regime) the SPE continua of the two components and is therefore *not* Landau damped by either plasma component. This nonexistence of AP Landau damping in the SPE ''gap'' regime in a 1D EHP is a fundamental one-dimensional effect arising from the suppression of long-wavelength single-particle excitations peculiar to 1D. We should mention, however, that,
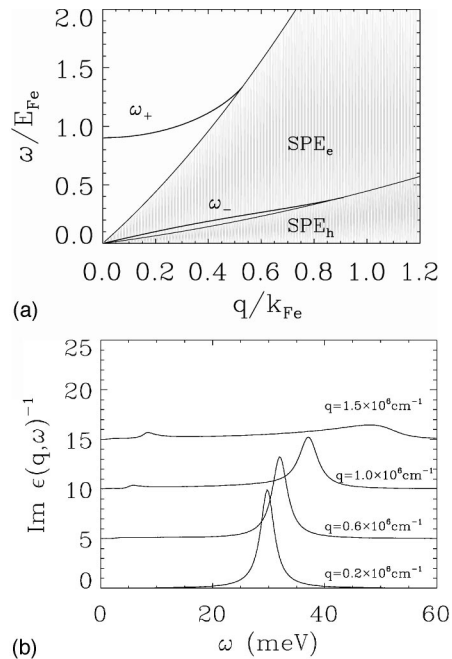

FIG. 9. The calculated (a) plasmon dispersions and (b) spectral weights for densities $n_e = n_h = 0.465 \times 10^{18}$ cm^{-3} in the photoexcited bulk GaAs EHP within RPA.

as is obvious from Figs. 5–7, inclusion of local-field corrections within the HA may push the AP mode down into the SPE continua of the higher mass plasma component, i.e., the hole SPE, making the AP mode strongly Landau damped even in the 1D EHP — our comparison between 1D and 2D/3D EHP collective modes and their qualitative difference are based on the RPA, going beyond RPA may very well render the 1D AP unobservably Landau damped as happens, for example, within the HA in our calculation for $n < 1.2 \times 10^6$ cm^{-1} in Figs. 5 and 6.

It is very anticlimactic, however, that even within the RPA the qualitative difference in the Landau damping behavior of the AP in the 1D EHP compared with its higher dimensional counterparts is not dramatically reflected in the mode spectral weight or the dynamical structure factor, as can be seen by comparing the RPA spectral weights in Figs. 5(b), 6(b), and 7(b) in the 1D EHP with those in the 2D/3D EHP given in Figs. 8(b) and 9(b). (We emphasize that we use equivalent impurity level broadening, $\gamma = 0.1 E_F$, in all our spectral weight calculations.) In general, the spectral weight carries by the AP mode (the lower-frequency peak in the dynamical structure factor Im$[\epsilon^{-1}]$ for each q) is comparable, albeit slightly larger, in the 1D EHP as that in the 2D/3D EHP. In particular, the AP spectral weights in the 1D and the 2D EHP seem to be quantitatively similar whereas the corresponding 3D AP mode carries considerably less spectral weight (which is understandable based on the fact that in 3D the OP has a finite gap at long-wavelengths in contrast with the 1D/2D OP which vanishes at long wavelengths, and therefore in a 3D EHP the long-wavelength OP mode carries considerably more relative spectral weight than its lower dimensional counterparts). The fact that the 1D AP carries small spectral weight in spite of its lack of Landau damping can be easily understood on the basis of the *f*-sum rule, which is essentially completely exhausted by the OP in the long-wavelength limit, leaving rather little spectral weight to be carried by the 1D AP in the long wavelength. At large wave vectors (i.e., away from the long-wavelength limit), on the other hand, the AP is Landau damped (because it enters the SPE continua) and all collective modes start carrying little spectral weights.

We therefore conclude this section on 1D EHP collective modes with two relatively modest conclusions: (1) In spite of the nonexistence of AP Landau damping in the 1D EHP within RPA, the calculated AP spectral weight is not much larger than the corresponding 2D situation (it is, however, substantially larger than the corresponding 3D situation), and therefore the observability of 1D EHP AP should be only slightly more favorable than the corresponding 2D case; (2) inclusion of local-field corrections in general severely suppresses the AP spectral weight in the 1D EHP, and at least within the HA the AP becomes unobservable at lower densities.

V. TWO-COMPONENT LUTTINGER LIQUID

In this section we briefly discuss, for the sake of completeness, the AP mode of the two-component Luttinger liquid, which has two different Fermi velocities v_{Fe} and v_{Fh} corresponding to the electron and the hole, respectively. We make the standard Luttinger model approximation of linear-

izing the single-particle energy. This system can be described by the two-component Luttinger model[26] Hamiltonian

$$H = \sum_{i,k,\sigma} v_{Fi} k [a^{\dagger}_{i,k,\sigma} a_{i,k,\sigma} - b^{\dagger}_{i,k,\sigma} b_{i,k,\sigma}]$$

$$+ \frac{1}{2L} \sum_{i,j,q} V_{i,j}(q) \rho_i(q) \rho_j(-q), \qquad (31)$$

where $i,j = e,h$, and $a_{i,k,\sigma}(b_{i,k,\sigma})$ is the destruction operator of the right- (left-) moving ith component with momentum k and spin σ, $V_{i,j}(q)$ the Coulomb interaction between ith and jth component (here $V_{i,j} = V_{ee} = V_{hh} = -V_{eh}$, and $\rho_i(q) = \rho_{i,a}(q) + \rho_{i,b}(q)$ the total density operator of the ith component.

By standard bosonization methods[20,26] we can diagonalize Eq. (31) and find two eigenmodes corresponding to the charge-density excitations:

$$\omega^2_{\pm}(q) = \frac{q^2 v^2_{Fe}}{2} [1 + \alpha^2 + (1+\alpha)\widetilde{V}(q)]$$

$$\pm \frac{q^2 v^2_{Fe}}{2} \{[1 + \alpha^2 + (1+\alpha)\widetilde{V}(q)]^2$$

$$- 4\alpha [\alpha + (1+\alpha)\widetilde{V}(q)]\}^{1/2}, \qquad (32)$$

where $\alpha = v_{Fh}/v_{Fe}$ and $\widetilde{V}(q) = 2V_{ee}(q)/(\pi v_{Fe})$; note that $V_{ee} = V_{hh} = -V_{eh}$ in the 1D EHP. In the long-wavelength limit, $q \to 0$, Eq. (32) becomes

$$\omega_+(q) = v_{Fe} q [1 + (1+\alpha)\widetilde{V}(q)]^{1/2}, \qquad (33)$$

$$\omega_-(q) = \sqrt{\alpha} q v_{Fe}. \qquad (34)$$

These long-wavelength charge-density modes defined by Eqs. (33) and (34) are exactly the same as the long-wavelength collective modes in the 1D EHP within RPA [Eqs. (29) and (30)]. This can be explained by the fact that vertex corrections to the irreducible polarizability of the 1D system vanish[9] in the Luttinger model, and therefore RPA and Luttinger model results become identical in the long-wavelength limit. Even though the charge-density mode dispersions of the Luttinger model are identical to the RPA collective-mode predictions based on the Fermi-liquid theory, the damping properties of the ω_- AP mode in the Luttinger model is strikingly different form the RPA result. In the previous section we found that within RPA the AP mode in the 1D EHP exists only at long wavelengths as the AP mode gets severely damped by Landau damping at finite wave vectors where it enters the electron single-particle continua and is Landau damped. However, since there are no equivalent SPE Landau damping mechanisms in the Luttinger model the AP mode in the Luttinger model seems not to be damped out even at the finite wave vectors, and seems to exist at arbitrary wave vectors.

The above-discussed difference between the RPA (Fermi-liquid) result and the Luttinger model (non-Fermi-liquid) result seems to suggest a direct experimental approach to observe the predicted non-Fermi-liquid-like behavior of a one-dimensional system by studying its plasmon damping

behavior which, according to the RPA (Luttinger) model, should (should not) manifest finite wave-vector Landau damping. This is, however, misleading because the strict nonexistence of any damping of the collective modes at any wave vectors is purely a result of the Luttinger *model* (rather than being a generic Luttinger *liquid* result), arising entirely from the linearization of the single-particle energy [the first term in Eq. (31)] in the Hamiltonian. In the generic Luttinger liquid behavior, where one does *not* linearize the single-particle energy, higher-order processes (which asymptotically vanish at low energies and long wavelengths) produce collective-mode damping arising from the (multiboson) boson-boson collision processes within the bosonized theoretical description. Such multiboson collision processes, which are akin to phonon-phonon anharmonic scattering processes producing phonon decay beyond the harmonic crystal theory, are *irrelevant* in the renormalization group sense at long wavelengths, but do produce damping of the collective modes at finite wave vectors. In this sense, therefore, no fundamental distinction exists between the two theoretical approaches since both predict damping of the collective modes at finite wave vectors, but *not* at zero wave vectors. One expects the AP damping in the Luttinger liquid theory to be a smooth function of wave vector q, vanishing only in the long-wavelength limit $q \to 0$. This seems to be drastically different from our RPA damping result where the AP is undamped upto a wave vector q_c when it becomes damped as it enters the SPE continuum. Going beyond RPA, however, one finds that the AP is damped even outside the SPE Landau damping continua due to multipair (i.e., multiple electron-hole excitations) productions, and therefore there may *not* be much qualitative difference between RPA and Luttinger liquid theories even for the AP damping properties. This issue, however, merits further investigations, and detailed theoretical calculations of the AP damping properties in the two-component Luttinger liquid may very well point to some significant differences with our RPA results, which then may lead to a direct method of differentiating between Luttinger liquid and RPA results, based on the experimentally measured damping properties. Very recently, such a calculation[27] has been carried out for a *one-component* clean Luttinger liquid using the *short-range* interaction which, however, has to be generalized to the realistic long-range Coulomb interaction in 1D quantum wires before any firm conclusion on the damping behavior contrast between RPA and Luttinger liquid may be reached. We emphasize that the AP damping property being manifestly a nonuniversal property (determined by irrelevant operators such as the band curvature), its actual quantitative calculation in the Luttinger liquid theory is problematic.

VI. SUMMARY

We have obtained the dispersion and spectral weight of collective charge-density excitations in zero-temperature two-component one-dimensional quantum plasma confined in semiconductor quantum-wire structures. In some sense this paper is a two-component generalization of our earlier work[15] where we studied the zero-temperature collective charge-density excitations of the one-component 1D system in some detail. In a separate earlier publication[14] we consider

a specific example of collective modes in a two-component 1D electron system (namely, a two-subband 1D system) in the context of obtaining quantitative agreement with the experimental results of Ref. 6. In the current paper we refrain from repeating any results from these earlier publications[14,15] of ours, and the current paper, along with Refs. 14 and 15, forms a reasonably complete quantitative description of possible low-lying collective charge-density excitations in 1D semiconductor quantum-wire structures.

Our main results in this paper are the following: (1) there are two possible collective charge-density excitations in a two-component 1D quantum plasma associated with the relative phase fluctuations in the two charge densities — the OP mode is the in-phase (out-of-phase) mode when the two components are the same (opposite) kind (both electrons or both holes versus one component electron and the other component hole) and the AP is the out-of-phase (in-phase) mode in the same situation (in general, the AP is essentially a neutral excitation at long wavelengths and the OP is the collective oscillation of the total charge density); (2) in contrast to higher dimensional systems where the AP mode is often Landau damped because it lies in the SPE continuum of the faster moving charge component, the 1D AP mode is invariably undamped at long wavelengths (within RPA) due to the severe suppression of long-wavelength SPE continua in 1D; (3) this RPA result of the nonexistence of long-wavelength Landau damping in the 1D AP mode is drastically affected by local-field corrections, which at low density may overdamp the AP mode by pushing it inside the SPE continua of both components—the OP mode, on the other hand, is relatively robust with respect to local-field corrections since its long-wavelength dispersion is fixed by the f-sum rule; (4) the AP mode in general carries little spectral weight at long-wavelengths, and even at finite wave vectors its spectral weight is only slightly enhanced with respect to the corresponding 2D two-component situation, leading to the somewhat disappointing and unexpected conclusion that in spite of the complete suppression of the long-wavelength SPE continua in 1D systems the neutral AP mode is not substantially easier to observe in 1D than in 2D/3D systems; (5)

finite interwire separation in general enhances the AP spectral weight increasing its observability; (6) finite impurity scattering induced level broadening gives rise to a critical wave vector below which the collective modes are always overdamped, and thus the concept of a long-wavelength collective mode does not strictly apply; (7) finite interwire tunneling produces a long-wavelength plasma gap in the AP mode; (8) Luttinger liquid theory and Fermi-liquid-based RPA theory produce formally identical OP and AP collective-mode behavior in 1D two-component systems making it impossible to observe any characteristic 1D Luttinger liquid signature in the collective charge-density excitation spectral in one dimension; (9) the AP mode being strongly (and qualitatively) affected by the local-field corrections (with the OP mode being relatively unaffected), in principle, it should be possible to investigate many-body effects in 1D systems by studying the dispersion and damping of the AP mode (the OP mode, on the other hand, should be relatively insensitive to these many-body corrections except at rather large wave vectors).

In our calculations we have concentrated on two distinct types of experimentally realizable two-component quasi-1D quantum plasmas confined in semiconductor (GaAs) quantum-wire nanostructures: spatially separated doped quantum double-wire structures and photoexcited homogeneous 1D EHP in a single wire. Both systems are potentially interesting from the perspective of 1D collective excitation spectra and provide somewhat complementary information. Our hope is that our detailed quantitative (both numerical and analytical) investigation of the collective-mode dispersion and spectral weight in two-component 1D system will motivate experimental work (involving inelastic light-scattering and far infrared frequency domain spectroscopies) on the subject searching for the 1D AP mode in quantum-wire structures.

ACKNOWLEDGMENTS

---

[1] For reviews see, e.g., *Nanostructures and Mesoscopic Systems*, edited by W. P. Kirk and M. A. Reed (Academic, New York, 1992); C. W. J. Beenakker and H. van Houten, in *Solid State Physics: Advances in Research and Applications*, edited by H. Ehrenreich and D. Turnbull (Academic, New York, 1991).

[2] T. Demel, D. Heitmann, P. Grambow, and K. Ploog, Phys. Rev. B **38**, 12 732 (1988); Phys. Rev. Lett. **66**, 2657 (1991); G. Hertel, H. Drexler, W. Hansen, A. Schmeller, J. P. Kotthaus, M. Holland, and S. P. Beaumont, Solid-State Electron. **37**, 1289 (1994).

[3] W. Hansen, J. P. Kotthaus, and U. Merkt, in *Semiconductors and Semimetals*, edited by R. K. Willardson and A. C. Beer (Academic Press, San Diego, 1992), Vol. 35.

[4] A. Pinczuk and G. Abstreiter, in *Light Scattering in Solids V*, edited by M. Cardona and G. Güntherodt (Springer, Berlin, 1989).

[5] T. Egeler, G. Abstreiter, G. Weimann, T. Demel, D. Heitmann, P.

Grambow, and W. Schlapp, Phys. Rev. Lett. **65**, 1804 (1990); R. Strenz, U. Bockelmann, F. Hirler, G. Abstreiter, G. Böhm, and G. Weimann, *ibid.* **73**, 3022 (1994); A. Schmeller, A. R. Goñi, A. Pinczuk, J. S. Weiner, J. M. Calleja, B. S. Dennis, L. N. Pfeiffer, and K. W. West, Phys. Rev. B **49**, 14 778 (1994).

[6] A. R. Goñi, A. Pinczuk, J. S. Weiner, J. M. Calleja, B. S. Dennis, L. N. Pfeiffer, and K. W. West, Phys. Rev. Lett. **67**, 3298 (1991); A. R. Goñi, A. Pinczuk, J. S. Weiner, J. M. Calleja, B. S. Dennis, L. N. Pfeiffer, and K. W. West, in *Phonons in Semiconductor Nanostructures*, edited by J. P. Leburton, J. Pascual, and C. S. Torres (Plenum, New York, 1993), p. 287.

[7] Q. P. Li and S. Das Sarma, Phys. Rev. B **43**, 11 768 (1991), and references therein.

[8] Q. P. Li, S. Das Sarma, and R. Joynt, Phys. Rev. B **45**, 13 713 (1992).

[9] I. E. Dzyaloshinskii and A. I. Larkin, Zh. Éksp. Teor. Fiz. **65**, 411 (1973) [Sov. Phys. JETP **38**, 202 (1974)].

[10] D. Pines, Can. J. Phys. **34**, 1379 (1956).

[11] A. Pinczuk, J. Shah, and P. A. Wolff, Phys. Rev. Lett. **47**, 1487 (1981), and references therein.

[12] S. Das Sarma and A. Madhukar, Phys. Rev. B **23**, 805 (1981); J. K. Jain and S. Das Sarma, *ibid.* **36**, 5949 (1987).

[13] B. Tanatar, Solid State Commun. **92**, 699 (1994); J. S. Thakur and D. Neilson, Phys. Rev. B **56**, 4671 (1997); N. Mutluay and B. Tanatar, J. Phys.: Condens. Matter **9**, 9819 (1997).

[14] E. H. Hwang and S. Das Sarma, Phys. Rev. B **50**, 17 267 (1994).

[15] S. Das Sarma and E. H. Hwang, Phys. Rev. B **54**, 1936 (1996).

[16] Ben Yu-Kuang Hu and S. Das Sarma, Phys. Rev. Lett. **68**, 1750 (1992); Phys. Rev. B **48**, 5469 (1993).

[17] G. F. Giuliani and J. J. Quinn, Phys. Rev. B **29**, 2321 (1984); S. Das Sarma and W. Y. Lai, *ibid.* **32**, 1401 (1985); J. G. Cordes and A. K. Das, Solid State Commun. **80**, 145 (1991).

[18] D. Z. Liu and S. Das Sarma, Phys. Rev. B **51**, 13 821 (1995).

[19] N. D. Mermin, Phys. Rev. B **1**, 2362 (1970).

[20] G. D. Mahan, *Many Particle Physics*, 2nd ed. (Plenum, New York, 1990).

[21] S. Das Sarma and E. H. Hwang, Phys. Rev. Lett. **81**, 4216 (1998).

[22] W. Wegscheider, L. N. Pfeiffer, M. M. Dignam, A. Pinczuk, K. W. West, S. L. McCall, and R. Hull, Phys. Rev. Lett. **71**, 4071 (1993).

[23] D. Pines and J. R. Schrieffer, Phys. Rev. **124**, 1387 (1961); P. M. Platzmann, *ibid.* **139**, A379 (1965).

[24] P. M. Platzmann and P. A. Wolff, *Waves and Interactions in Solid State Plasma* (Academic, New York, 1973), Chap. 5; M. V. Klein, in *Light Scattering in Solids I*, edited by M. V. Cardona (Springer, Berlin, 1975), p. 147; J. Ruvalds, Adv. Phys. **30**, 677 (1981).

[25] I. Alexeff and R. V. Neidigh, Phys. Rev. **129**, 516 (1961).

[26] F. D. M. Haldane, J. Phys. C **14**, 2585 (1981).

[27] K. V. Samokhin, J. Phys.: Condens. Matter **10**, L533 (1998).